J Seismol (2009) 13:415–420
DOI 10.1007/s10950-008-9111-5

ORIGINAL ARTICLE

GPS measurements of postseismic deformation due to October 8, 2005 Kashmir earthquake

C. D. Reddy · Sanjay K. Prajapati

Received: 13 February 2008 / Accepted: 8 May 2008 / Published online: 17 June 2008
© Springer Science + Business Media B.V. 2008

Abstract Relaxation of the coseismic stresses following an earthquake causes postseismic crustal deformation, which can last for days to years. Continuous monitoring of postseismic deformation facilitates the understanding of the mechanism of deformation and postseismic relaxation and viscous rheology. After the October 8, 2005 Kashmir earthquake, global positioning system data for 8 months, starting from October, 2005 have been analyzed from three continuous sites located at Gulmarg, Amritsar, and Jaipur. The average velocity during the observation period at Gulmarg (8.6 cm/year) is significantly higher than the Indian plate velocity exhibiting postseismic crustal deformation. The velocity at Amritsar (5.9 cm/year) and Jaipur (5.1 cm/year) is comparable to the Indian plate velocity. At Gulmarg, the logarithmic function fits well to the north–south component of postseismic transients (∼in the coseismic slip direction). The nature of decay in these transients suggests that the deformation is mainly due to an afterslip, and the second possible contribution may be from the viscous relaxation process. This paper presents the characteristics of postseismic transients and possible contributions from various postseismic mechanisms subsequent to the Kashmir earthquake.

Keywords GPS · Postseismic deformation · Afterslip · Logarithmic decay

1 Introduction

Understanding the seismo-tectonic process requires detailed insight into how the tectonic stresses are accumulated and released in seismogenic regions. Large earthquakes cause changes in stress distribution in the environing crust such that some places have a reduction in stress (stress shadows) and other places have an increase in stress (stress halos). The places of increased stress are important, and it is these regions where aftershocks occur obeying Omori's modified law (Shcherbakov et al. 2004). The relaxation of this stress takes place at these regions and may cause crustal deformation for months to years after a major earthquake. This relaxation manifests as a time-dependent mechanical response of the host rocks to the coseismic stress changes. Thus, the analysis of postseismic deformation provides information on rheological and constitutional properties of the lower crust and upper mantle. There are many possible mechanisms of postseismic

C. D. Reddy (✉) · S. K. Prajapati
Indian Institute of Geomagnetism,
New Bombay 410218, India
e-mail: cdreddy@iigs.iigm.res.in

deformation. Three of the most accepted are: afterslip (via either velocity strengthening frictional slip or linear viscous creep; Shen et al. 1994; Savage and Svarc 1997), visco-elastic relaxation (Deng et al. 1998), and poro-elastic relaxation (occurs in the upper crust; Peltzer et al. 1996). The major difference between the first two mechanisms is that the afterslip is localized, while visco-elastic relaxation is a bulk deformation process. The afterslip represents a fundamental physical process of a fault zones (Marone et al. 1991). Though many empirical relations could explain the afterslip curves, they cannot yield to any underlying physical mechanisms.

The October 8, 2005 Kashmir earthquake (7.6 M_w) in the Indus Kohistan Seismic Zone is a major seismic event in the Himalaya region (Rao et al. 2006). The earthquake occurred along a tectonic boundary, which is characterized by high seismic activity. The epicenter lies in the Kishanganga valley, in the Frontal Himalayan belt, and bounded by Main Boundary thrust and Jhelum fault. The focal mechanisms from Harvard and US Geological Survey show that the earthquake was predominantly of a thrust type. The large ground upheaval along Muzaffarabad and Tanda faults suggests that these active faults are responsible for the destructive earthquake. The surface rupture of about 70 km occurred along these faults (Avouac et al. 2006). Both the global positioning system (GPS) and synthetic aperture radar (ENVISAT; Pathier et al. 2006) were used to find the distribution of coseismic displacement (Bendick et al. 2007; Avouac et al. 2006; Pathier

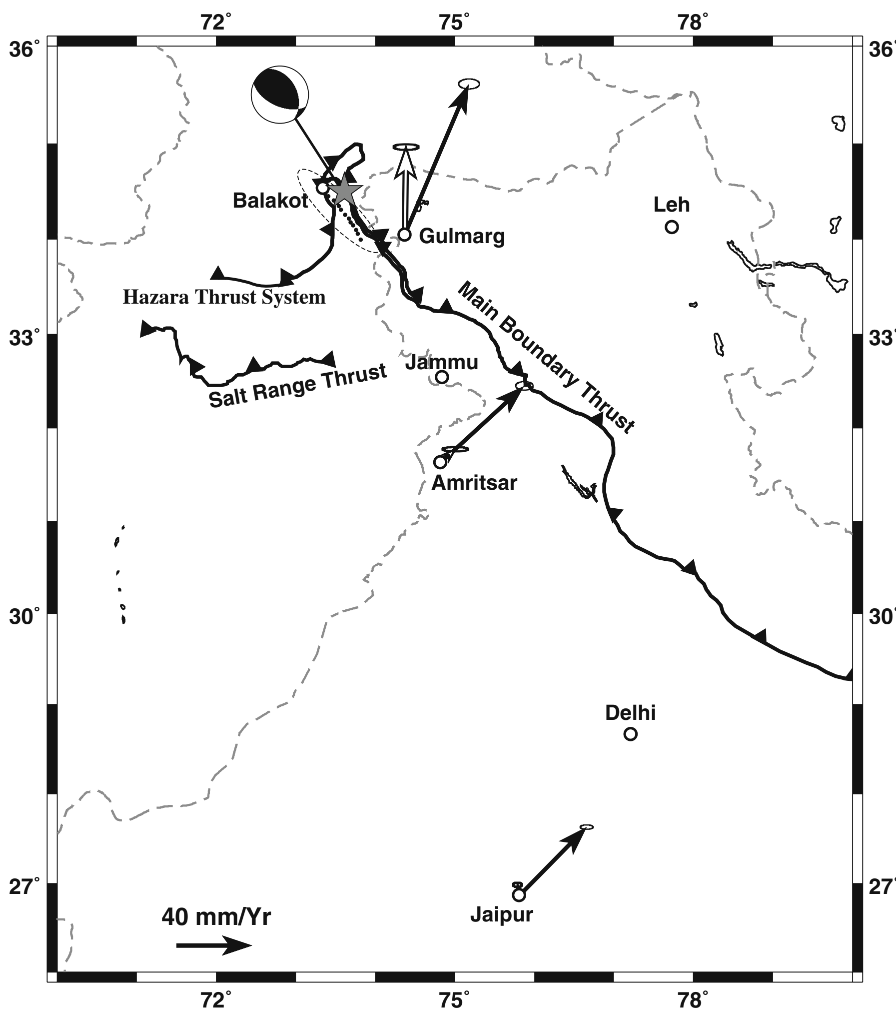

Fig. 1 Velocity vectors with 95% confidence level at three continuous GPS sites, Gulmarg, Amritsar, and Jaipur (*solid*—ITRF2000, *open*—relative to Indian plate). Fault plane solution of main shock shows the northeast–southwest compressional regime north of Gulmarg. The *dotted line enclosed by ellipse* indicates the surface rupture zone. More details of this rupture are given by Avouac et al. (2006). *Star* indicates the epicenter of the Kashmir earthquake

et al. 2006). Various studies arrived at maximum coseismic slip of about 6 m (e.g, Avouac et al. 2006; Pathier et al. 2006; Wang et al. 2007). Immediately after the earthquake, we initiated GPS measurements in the Jammu and Kashmir regions to constrain possible mechanisms of postseismic deformation and to examine the possible tectonic processes associated with the Kashmir earthquake. Spatially varying rheological parameters (Montesi 2003), particularly the viscosity structure of the mantle, play a major role in the far-field postseismic deformation (at distances from the epicenter of the order of 100 km; Sabadini and Vermeersen 1997; Piersanti et al. 1995). To study the near and far-field postseismic crustal deformation, we have established three continuous GPS stations at Gulmarg (GUMR), Amritsar (AMRT), and Jaipur (JAPR; shown in Fig. 1) at varying distances from the epicentral area (to the southeast of it, parallel to the rupture propagation).

2 GPS data collection and analysis

Continuous GPS data have been collected (at a 30-s sampling interval, 15° angle of elevation) at three sites, viz., GUMR, AMRT, and JAPR (Fig. 1). GUMR is the closest site to the epicenter, i.e., ~70 km, and can facilitate the studying of the near-field postseismic deformation. At this site, there was loss of some data due to heavy snowfall during winter. At AMRT and JAPR, continuous data have been recorded. We have also included one site from Indo-Gangetic Plains namely, Allahabad (ALHA). We used the nearby International GPS Service (IGS) sites, viz., IISC, HYDE, BAHR, KIT3, and LHAS, and tightly constrained the site coordinates to ITRF2000.

GPS data for 8 months, i.e., starting from October, 2005, have been used for the analysis. The data were organized into 24-h segments (i.e., 00:00 universal time [UT] to 23:59 UT). Precise orbits and Earth rotation parameters from IGS were used. The position and baseline time series are estimated in ITRF2000 using GAMIT/GLOBK software (King and Rock 2000). The east–west (EW) and north–south (NS) components of

Table 1 The horizontal velocity components (EW and NS, in ITRF2000) at four local sites and also shown relative to the Indian plate (Indian plate velocity is taken from Bettinelli et al. (2006)

Station	*X*(E), mm/year	Root mean square error, *X*(E) in mm	*Y*(N), mm/year	Root mean square error, *Y*(N) in mm	*X*(E) relative to Indian plate	*Y*(N) relative to Indian plate	Day of the year (DOY)
GUMR	33.72	5.03	79.15	2.40	0.48	45.76	342–585
AMRT	44.05	4.19	40.37	2.06	9.62	6.96	293–418
JAPR	35.31	3.13	35.89	1.04	−1.27	2.44	298–480
ALHA	46.74	3.41	23.44	0.06	8.12	−10.01	308–418

DOY indicates the duration of data used for the analysis

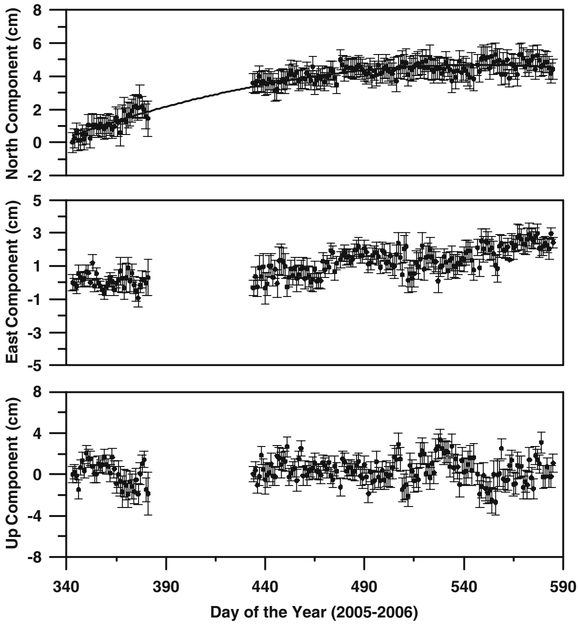

Fig. 2 The time series of the position coordinates (EW, NS, and UD components) at the site Gulmarg (GUMR). Logarithmic decay is seen in the NS component. The data gap is due to heavy snow fall during winter

velocity at four local sites are given in Table 1 and presented in the form of vectors in Fig. 1.

Further, the components (NS, EW, and up–down [UD]) of the position coordinates are obtained using all available data, and their time series are ploted in Fig. 2 (for GUMR) and Fig. 3 (for AMRT and JAPR). It is clear from Fig. 2 that at GUMR, the NS component of the time series exhibits clear postseismic deformation. A logarithmic decay of the form $y = a \log\left[b\,(x - 62) - 1\right]$ is considered to fit the data. As the data have been considered from the 62nd day after the earthquake, the number 62 is used in the above relation. We could not fit either the exponential or logarthimic function to EW and UD components.

3 Results and discussion

As seen from Fig. 1, during the observation period (October, 2005 to July, 2005), the site GUMR is moving with velocity 8.6 cm/year. The velocity at the sites AMRT (5.9 cm/year), JAPR (5.1 cm/year), and ALHA (5.2 cm/year) is in conformity with the general trend of the Indian plate motion. The discrepancy in the velocity at the latter three sites is due to the short duration of the GPS observations. The velocity at GUMG may contain contributions from at least three processes, (1) The plate motion at this site, (2) contribution from interseismic strain accumulation, and (3) contribution from postseismic relaxation due to the 2005 Kashmir earthquake. Assuming that the other two sites are away from the source region, the average of AMRT and

Fig. 3 The time series of the position coordinates (EW, NS, and UD components) at the sites Amritsar (AMRT, *left*) and Jaipur (JAPR, *right*). The time series characteristics are in compliance with the Indian plate motion

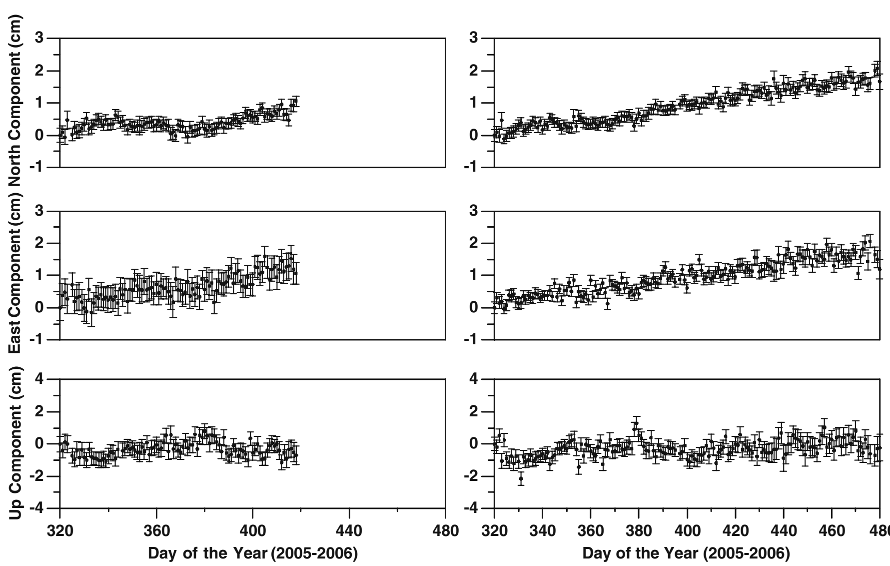

JAPR (5.5 cm/year) represents the first contribution, and subtracting this velocity from GUMR will approximately yield postseismic and interseismic strain accumulation deformation (about 3.3 cm in 8 months). However, interseismic strain accumulation contribution will be of opposite polarity than that of the postseismic strain and is unknown. Thus, the estimated deformation rate of 3.3 cm/year at GUMR will correspond to the lower-bound estimate of the postseismic deformation. Jouanne et al. (2006) reported the occurrence of centimetric postseismic displacement with a maximum at the GPS site just north of Balakot (shown in Fig. 1). Further, as discussed below, the logarithmic transient decay also implies that it is postseismic deformation.

The stress change associated with this earthquake is significant enough to cause observable transient crustal deformation. As already discussed, several stress transfer mechanisms, viz., afterslip, visco-elastic relaxation, and poro-elastic relaxation, can be involved in postseismic deformation. However, based on the following reasons, it is inferred that the deformation mechanism could be due to the aseismic afterslip: (1) A long-wavelength postseismic signal following the logarithmic function, i.e., the afterslip, obeys the state variable friction laws (Scholz 1998) and is governed by the interaction between a velocity-weakening zone over the coseismic rupture and a velocity-strengthening zone below it (down dip; Savage et al. 2005) with decay time of about 96 days (visco-elastic relaxation cannot account for rapid transient relaxation), and (2) a higher heat flow is a signature of a higher crustal temperature, which leads to larger strain relaxation by the creep/afterslip. High heat flow and geothermal gradients of 140–468 mW/m^2 and 234°C/km, respectively, have been reported from the Kashmir region (Panda et al. 2007; Ravi Shanker 1988). The above mentioned afterslip is via a velocity-strengthening frictional slip. Many faults exhibit velocity-strengthening frictional behavior (i.e., frictional resistance increases with slip velocity; Marone et al. 1991), and Muzaffarabad/Tanda faults may not be an exception.

The relaxation is seen maximum in the NS direction when compared to EW direction. While the north component of the position time series at GUMR clearly portrayed the logarithmic postseismic decay, EW and UD components could not be fitted either to the logarithmic or exponential functions. Generally, the postseismic slip due to the relaxation process at shallow depth decays more rapidly with time than at greater depths. As the decay time is very less when compared to the areas such as the Andaman region (Ohta et al. 2006), we may infer that the afterslip region is at a shallow depth. The low-viscosity zone beneath the lithosphere also may be one of the reasons for the faster relaxation. Postseismic deformation of the Kashmir earthquake seems to confine to the 100–200 km around the epicenter. This is evident from the characteristics of time series of the position coordinates at AMRT and JAPR (Fig. 3) where no postseismic deformation was observed at these sites.

4 Conclusions

After the 2005 Kashmir earthquake, three continuous GPS sites have been set up at GUMR, AMRT, and JAPR. During October, 2005 to June, 2006, the velocity at GUMR (southeast of the rupture zone) is 8.6 cm/year, which is significantly higher than the Indian plate velocity indicating near-field shallow postseismic crustal deformation. At this site, postseismic displacements of at least 3.3 cm is observed in the first 8 months, and the time series of the position coordinates exhibited northward, logarithmically decaying postseismic deformation. The characteristic of this deformation indicates that the velocity-strengthening frictional afterslip is the likely cause. The afterslip can lead to an increase in stress in certain regions of the upper crust, potentially loading nearby faults (Freed 2005). Data from a longer duration can facilitate the delineation of other contributions such as visco-elastic and poro-elastic ones.

Acknowledgements We thank our colleagues Dr. P.S. Sunil, Mr. Ajay Dhar, and Dr. Subba Rao for their help in setting up the GPS sites. We thank Dr. Khan and Mr. Vijay of Jaipur magnetic observatory for maintaining a permanent GPS site. We thank Prof. Surendra Singh, Mr. Arvind, and Mr. Mahajan, Department of Physics, Gurunank University, Prof. Lalmani Singh, Engineering

College, Jammu, for providing all required logistics to install the GPS receivers in their premises. We thank anonymous reviewer for his suggestions/comments, which improved the manuscript. We thank Prof. Bob King for his GAMIT/GLOBK program and certain clarifications. We thank Dr. Vineet Gahalaut for his suggestions and for improving the manuscript. We thank Prof. Archana Bhattacharyya for her encouragement.

References

Avouac JP, Ayoub F, Sebastien L, Ozgun K, Helmberger DV (2006) The 2005, M_w 7.6 Kashmir earthquake: sub-pixel correlation of ASTER images and seismic waveforms analysis. Earth Planet Sci Lett 249:514–528

Bendick R, Bilham R, Asif Khan M, Faisal Khan S (2007) Slip on an active wedge thrust from geodetic observations of the 8 October 2005 Kashmir earthquake. Geology 35:267–270

Bettinelli P, Avouac JP, Flouzat M, Jouanne F, Bollinger L, Willis P, Chitrakar GR (2006) Plate motion of India and interseismic strain in the Nepal Himalaya from GPS and DORIS measurements. J Geod 80:567–589

Deng J, Gurnis M, Kanamori H, Hauksson E (1998) Viscoelastic flow in the lower crust after the 1992 Landers earthquake, California. Science 282:1689–1692

Freed AM (2005) Earthquake triggering by static, dynamic, and post-seismic stress transfer. Annu Rev Earth Planet Sci 33:335–367

Jouanne F, Latif M, Majid A, Kausar A, Pécher A, Mugnier JL (2006) Current shortening across the Himalayas: quantification of interseismic deformation in Nepal and first results of postseismic deformation in Pakistan after the 8th October earthquake. Available at: http://lgca.obs.ujf-grenoble.fr/perso/jlmugnie/publications/2006FJICASTPakistan.pdf

King RW, Bock Y (2000) Documentation for the GAMIT GPS analysis software, release 10.0. MIT, Cambridge, MA

Marone CJ, Scholz CH, Bilham R (1991) On the mechanism of earthquake after slip. J Geophys Res 96:8441–8452

Montesi LGJ (2003) Inferring shear zone rheology from the time dependence of postseismic deformation. Available at: http://www.whoi.edu/science/GG/people/lmontesi/POSTERS/DRT2003.pdf

Ohta Y, Irwan M, Ito T, Kimata F, Tabei T, Sagiya T, Sugiyanto D (2006) Afterslip distribution following the 2004 Sumatra–Andaman earthquake in the northern Sumatra Segment based on the near field GPS data. In: Proceedings of the international joint workshop on comprehensive understandings of the 2004 Sumatra earthquake/tsunami and its affections, Syiah Kuala University, Darussalam, Banda Aceh, Indonesia

Panda SK, Saraf AK, Choudhury S, Das JD (2007) Thermal anomaly precedes major earthquake– a case study of 08 October 2005 Kashmir earthquake. In: Proceedings of the Asian seismological conference, symposium on earthquake and tsunami disaster preparedness and mitigation, 2006, Bangkok

Pathier E, Fielding EJ, Wright TJ, Walker R, Parsons BE, Hensley S (2006) Displacement field and slip distribution of the 2005 Kashmir earthquake from SAR imagery. J Geophys Res 33:L20310

Peltzer G, Rosen P, Rogez F, Hudnut K (1996) Postseismic rebound in fault step-over caused by pore fluid flow. Science 273:1202–1204

Piersanti A, Spada G, Sabadini R, Bonafede M (1995) Global post-seismic deformation. Geophys J Int 120:544–566

Rao NP, Kumar P, Kalpana, Tsukuda T, Ramesh DS (2006) The devastating Muzaffarabad earthquake of 8 October 2005: new insights into Himalayan seismicity and tectonics. Gondwana Res 9:365–378

Sabadini R, Vermeersen LLA (1997) Influence of lithospheric and mantle stratification on global post-seismic deformation. Geophys Res Lett 24:2075–2078

Savage JC, Svarc JL (1997) Postseismic deformation associated with the 1992 Mw = 7.3 Landers earthquake, Southern California. J Geophys Res 102:7565–7577

Savage JC, Svarc JL, Yu SB (2005) Postseismic relaxation and transient creep. J Geophys Res 110:B11402

Scholz CH (1998) Earthquakes and friction laws. Nature 391:37–42

Shanker R (1988) Heat-flow of India and discussion on its geological and economic significance. Indian Miner 42:89–110

Shcherbakov R, Turcotte DL, Rundle JB (2004) A generalized Omori's law for earthquake aftershock decay. Geophys Res Lett 31:L11613

Shen ZK, Jackson DD, Feng Y, Cline M, Kim M, Fang P, Bock Y (1994) Postseismic deformation following the Landers earthquake, California, 28 June 1992. Bull Seismol Soc Am 84:780–791

Wang H, Ge L, Xu C (2007) 3-D coseismic displacement field of the 2005 Kashmir earthquake inferred from satellite radar imagery. Earth Planets Space 59:343–349